Journal of Industrial Technology 15 (1), 2006, 1-10

FATIGUE MECHANISM OF SEMI-METALLIC BRAKE PADS DURING BRAKING PROCESS

R.J. Talib[1], A. Muchtar[2] and C.H. Azhari[2]

[1]AMREC, SIRIM Berhad, Lot 34, Jalan Hi-Tech 2/4,
Kulim Hi-Tech Park, 09000 Kulim, Kedah D.A

[2]Department of Mechanical and Materials Engineering,
Faculty of Engineering, Universiti Kebangsaan Malaysia,
43600 Bandar Baru Bangi, Selangor D.E.
(talibria@sirim.my)

RINGKASAN *: Mekanisme haus lesu didapati beroperasi semasa kedua-dua proses pembrekan mod terputus-putus dan berterusan. Dalam kajian ini, sepasang pad brek ditekan ke atas piring brek diperbuat dari besi tuang kelabu yang berpusing dengan kelajuan yang dietapkan pada 750 psm, simulasi keadaan pembrekan. Di dalam ujian mod pembrekan terputus-putus, sampel ujian dikenakan beban kenaan 600 N dengan empat jumlah masa pembrekan yang berlainan (400, 800, 1200 dan 1600 saat). Brek dikenakan untuk empat masa berlainan (5, 10, 15, dan 20 saat) sebanyak 80 kali dengan melahu 5 saat di antara setiap pembrekan. Sementara, dalam pembrekan terus, sampel ujian dikenakan lima masa pembrekan berlainan (180, 360, 540, 720 dan 900 saat) dan beban kenaan (100, 200, 400, 600 dan 800 N). Perubahan mikrostruktur ke atas permukaan haus diperhatikan menggunakan Kemikroskopan Imbasan Elektron (KEI). Pemeriksaan mikrostruktur menunjukkan mekanisme lesu bermula dengan penjanaan perubahan plastik di subpermukaan pad brek. Apabila masa pembrekan ditingkatkan, fenomena di atas menyebabkan pembentukan jejalur di atas permukaan haus pad brek. Pembrekan seterusnya, diperhatikan mekanisme lesu nukleus di kawasan di mana terdapat lubang dan serpihan. Akhirnya, serpihan haus tersingkir dari permukaan haus.*

ABSTRACT : Fatigue wear mechanism was found to operate during braking process both during intermittent and continuous braking modes. In this study, a pair of brake pads was pressed against a rotating cast iron brake disc at a constant rotating speed of 750 rpm, simulating braking condition. In the intermittent braking test mode, the test samples were subjected to an applied load of 600 N for four different total braking times (400, 800, 1200 and 1600 seconds). The brake was applied for four different times (5, 10, 15 and 20 seconds) for 80 times with idling 5 seconds between each braking. Whereas, in the continuous braking, the test samples were subjected to five different braking times (180, 360, 540, 720 and 900 seconds) and applied loads (100, 200, 400, 600 and 800 N). The microstructural changes on the wear surface were observed using Scanning Electron Microscopy (SEM). Microstructural examinations showed that the fatigue mechanism started with the generation of plastic deformation in the subsurface of the brake pads. As the braking time increased, the above phenomena caused the formation of striations on the worn surface of the brake pad. With subsequent braking, the fatigue mechanism was observed to nucleate at areas where pits and spalls were present. Finally, the wear fragments were disposed from the worn surface.

KEYWORDS : Brake pad, striation, microcrack, fatigue, wear

INTRODUCTION

Previous studies showed that the wear mechanisms operating during braking process were of types adhesion, abrasion, fatigue, delamination and thermal. Bros and Scieszka (1977) reported that the predominant wear mechanisms operating during the braking process were abrasion, adhesion and thermal. In another study on the asbestos-reinforced friction materials, Rhee (1974) observed the abrasive and adhesive wear mechanisms at low temperatures (below 230°C) and the pyrolysis mechanism at high temperatures during braking. Talib (1996, 2001) observed the abrasion, adhesion, fatigue, delamination, and thermal wear mechanisms operating during the intermittent braking and continuous braking processes of semi-metallic automotive friction materials.

The surface of engineering materials is rough in micro scale. Even after 400 seconds braking, the surface of friction materials is still rough with a roughness of 38.3 μm to 82.1 μm (Talib *et al.* 2002). The unevenness of the brake disc surface may cause the peak asperities to be subjected to cyclic contact. After repeated contact, fatigue microcracks will be generated at the point of maximum stress and minimum local strength (ASM, 1992). These microcracks can propagate and grow due to repeated normal and tangent shear during sliding. Symptoms of fatigue wear are noticeable by the appearance of wear surface in the form of striations, pits, spalls and microcracks. Bayer and Schumacher (1968) proposed that at the beginning of fatigue mechanism, striations are generated. This is followed by the formation of cross-hatching as the sliding increased. The formation of the cross-hatching is related to the propagation of the subsurface microcracks to the surface. The generation of the fatigue microcracks increased when the applied stress is more than 0.5 of yield stress. It also increased with an increase in the number of sliding.

Repeated sliding or rolling can result in cyclic stress at the contact region. This cyclic stress can initiate cracks at the contact region. There are three locations where microcracks can nucleate in the fatigue mechanism; (i) fatigue slip bend, (ii) grain boundaries, and (iii) surface inclusion (Klensil and Lukas, 1980). Their research also indicated that these fatigue microcracks are located along the slip plane having the maximum shear stress. With subsequent cyclic load, the microcracks propagate, grow and finally join each other. They also found that with increase in length, the growing microcracks leave the original location near the 45° – oriented slip planes and tend to propagate perpendicular to the stress axis. This transition is often called the transition from Stage I (crystallographic propagation) to Stage II (non-crystallographic propagation). In stage II of fatigue crack propagation, only one crack is usually propagating.

Bayer (1994) in his study on the sliding of copper observed that there are three stages of fatigue mechanism. In the first stage, grooves and striations in the direction of sliding are the predominant feature. Here no material is removed from the surface. In the second stage,

damage features perpendicular to the sliding direction appeared, termed as cross-hatching. Again, no material loss is observed. As sliding proceeds, the cross-hatching become more pronounced until ultimately spalling and flaking occurs. In this stage, material loss occurs. In the third stage, microcracks propagate and generate wear particles. The start of this stage is considered the end of the incubation period.

In this study, a postulate of the fatigue mechanism in semimetallic brake pad during the braking process is made based on the observation of microstructural changes occurring on the surface and subsurface of wear surfaces. The changes were observed using scanning electron microscopy (SEM).

MATERIALS AND METHODS

Four samples of different models and makes were used in this study and marked as A, B, C, and D. Samples A, B, C and D were used in intermittent braking while only sample D was used in the continuous braking test. All samples were subjected to friction tests as previously described in an earlier published paper (Talib & Azhari, 1997, 2000). The friction tests were conducted using a Schenck friction materials test machine. Figure 1 shows the layout of the friction test machine. Technical specification of the test machine is shown in Table 1. Test samples were cut from the brake pad backing plate with dimensions of $20 \pm 1 \times 30 \pm 1 \times 15 \pm 1$ mm as per specification of the friction machine. The samples were glued to the backing plate and placed in the oven at 180°C for one hour to ensure that the adhesive is properly cured. This backing plate was then attached to the brake callipers on both sides of the brake disc. When the brake was applied, a piston attached to the brake callipers pressed the test samples against a rotating brake disc.

Table 1. Technical specification of the test machine

Item	Specification
Machine model	Schenck friction test machine
Power	75 kw
Brake disc diameter	300 mm
Brake disc material	cast iron
Hardness	190 - 220 HB
Roughness	4.9 - 7.4 μm

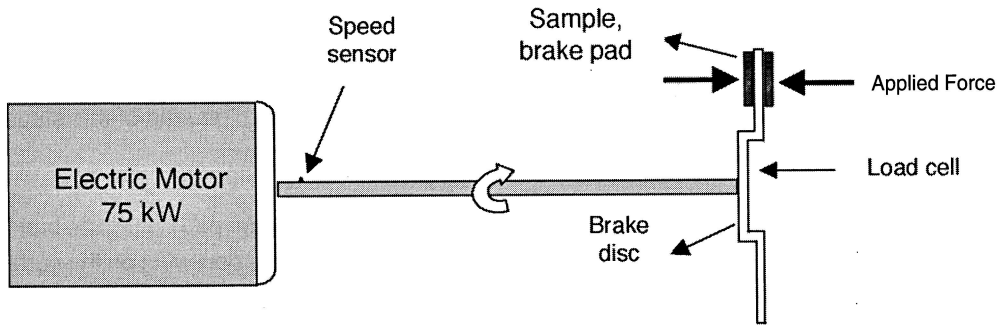

Figure 1. *Friction Test Machine Layout*

In continuous braking, each sample was subjected to five different braking times of 180, 360, 540, 720 and 900 seconds and applied loads of 100, 200, 400 and 600 N. On the contrary, the samples tested in intermittent braking were subjected to four different total braking times of 400, 800, 1200 and 1600 seconds and an applied load of 600 N. In this intermittent braking, the brake was applied for 80 times. In between braking, the brake was in the OFF position for 5 seconds. The brake was set to four different braking times of 5, 10, 15 and 20 seconds. Details of the intermittent braking procedures can be referred to an earlier published paper (Talib & Azhari, 1997). The rotating velocity of the brake disc in both cases was kept constant at 750 rpm (40 km/hr) for both continuous and intermittent braking modes.

After each test, the morphological changes on the surface and the subsurface were observed using a Scanning Electron Microscope (PHILIP SL 300). Samples for surface examination were cut from the backing plate, cleaned with compressed air and then coated with gold. Samples for subsurface examination were further cut parallel and perpendicular to the sliding surface using a fine cutter. The samples were mounted and polished to a surface finish of 1 μm.

RESULTS AND DISCUSSION

Microstructural examination of the subsurface and surface of the worn brake pads revealed the fatigue wear mechanism operated both during intermittent and continuous braking modes. In the early stages, fatigue microcracks were generated by the formation of striations. Our earlier study on the surface roughness of the brake pads showed that the surface of the friction materials were still rough even after a braking time of 1600 seconds with a surface roughness of 33.6 μm (Talib & Azhari, 1997). The unevenness of the brake disc could have caused the peak asperities on the brake pad being subjected to cyclic contact during braking

process. This phenomenon resulted in the generation of the plastic deformation in the subsurface of the brake pads. This deformation can be observed under SEM (Figure 2). With subsequent braking, the plastic deformation resulted in the generation of striations as observed in Figures 3 and 4. The generation of the striations is a symptom of fatigue wear mechanism. This was observed both during the intermittent and continuous braking modes.

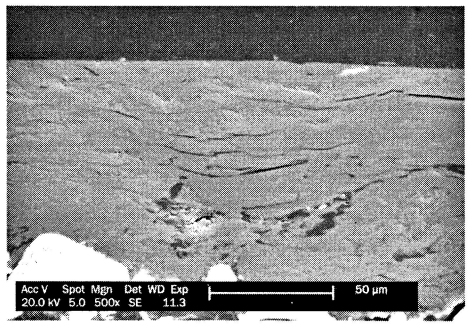

Figure 2. *Micrograph shows a number of deformation bands parallel to the wear surface under applied load of 100 N and braking time of 9 minutes*

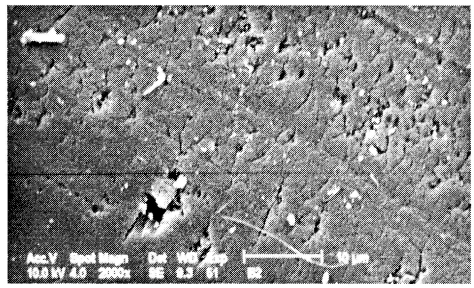

Figure 3. *Striations first appear on second braking (800 seconds) during intermittent braking under applied load of 600 N*

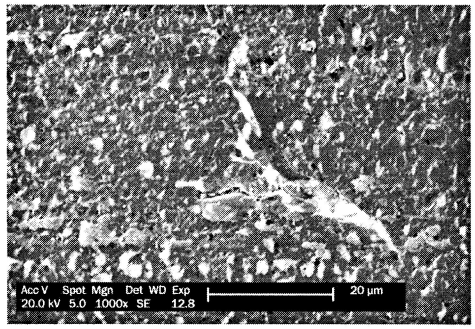

Figure 4. *The appearance of striations on the second braking (360 second) during continuous braking under applied load of 100 N*

The generation of the striations on the automotive friction materials depended on the type of braking (intermittent or continuous mode), applied loads and braking times used. Microstructural examination revealed that the striations first appeared during second braking for both intermittent (800 seconds) and continuous braking (360 seconds) modes but appeared at different braking time and applied load. Under intermittent braking, it first appeared under the applied load of 600 N and braking time of 800 seconds (Figure 3). The spacing between the striations became larger as the braking time was increased under the intermittent braking mode (Figure 4). Under continuous braking, however, striations were first observed during a braking time of 360 seconds with applied loads of 100 and 200 N (Figure 5). It was observed that the distance between the striations was rather small at the early stage of striation formation and the spacing became larger as the braking time increased (Figure 6). When the applied load was increased to 400 N, the generation of the striations started earlier i.e. at a braking time of 180 seconds (Figure 7). The spacing between the striations was noticeably larger (Figure 8). When the applied load was increased to 600 N, no striations were generated under this condition.

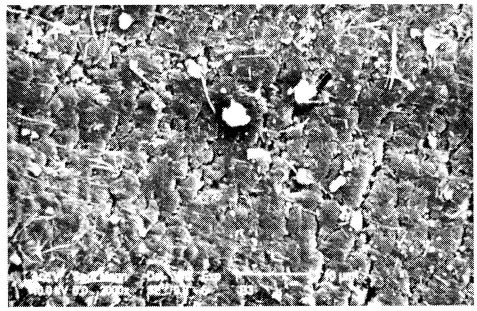

Figure 5. *The distance betweem the striations increases as the braking time increased during intermittent braking. Applied load 600 N and total braking time 1,200 seconds*

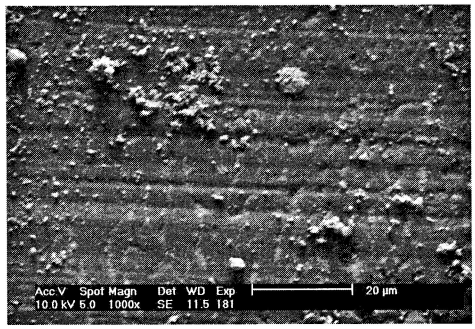

Figure 6. *Striations appear on the second braking during continuous braking. Applied load 200 N, 360 seconds*

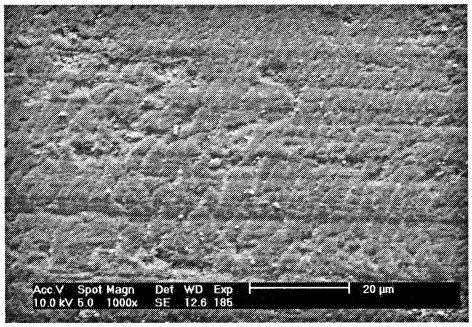

Figure 7. *The distance between the striations increases as the braking time increased to 540 seconds under applied load of 200 N during continuous braking*

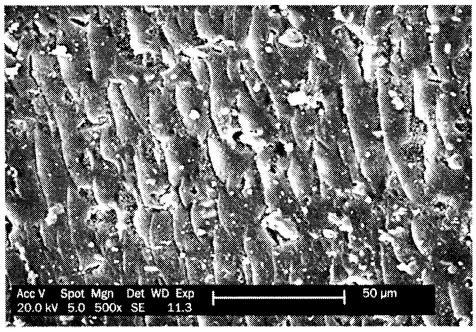

Figure 8. *The gap between the striations become larger and appeared at earlier braking time of 360 seconds when the applied load was increased to 400 N under continuous braking*

With subsequent braking, the fatigue microcrack propagated from stage I to stage II (Figure 9). In this stage only one microcrack appeared while others have stopped. This observation agreed with the finding of Klensil & Lukas (1980). As the braking time increased, the fatigue microcracks were observed to nucleate at the edges of transfer layer (Figure 10) or at the areas where pits and spalls were found (Figure 11). The generation of fatigue microcracks were observed both in the intermittent and continuous braking mode. With subsequent braking, the microcracks eventually propagated, grew and joined each other to form loose particles. In intermittent braking, the fatigue microcracks operated when the braking time was below 1,200 seconds with the applied load of 600 N (Figure 12). On the other hand, during continuous braking, the fatigue microcracks were observed when the applied load was less than 400 N and this mechanism was first observed at a braking time of 720 seconds under the applied load of 100 N (Figure 13). When the applied load was increased to 200 N, fatigue microcracks were generated earlier at a braking time of 540 seconds.

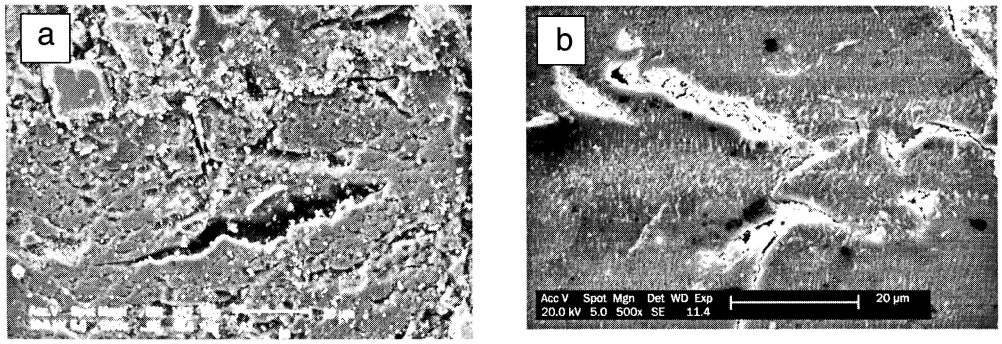

Figure 9. *Micrograph shows stage II fatigue microcrack*
(a) Intermittent braking
(b) Continuous braking

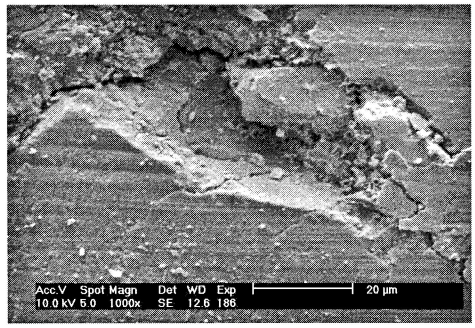

Figure 10. *Fatigue microcrack in the middle of the plate under continuous braking. Applied load of 200 N, braking time 540 seconds*

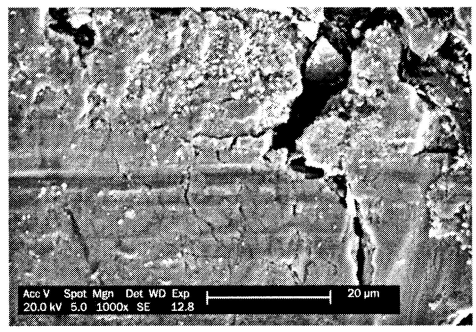

Figure 11. *Fatigue microcrack formation at the edge of the transfer layer under continuous braking. Applied load 200 N, braking time 720 seconds*

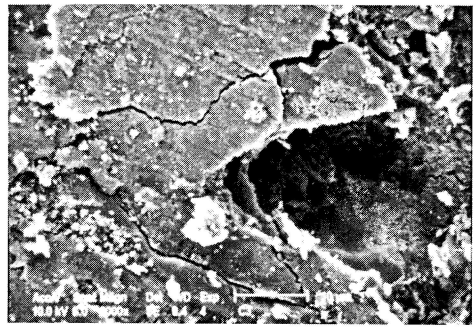

Figure 12. *The appearance of fatigue microcrack during intermittent braking. Applied load 600 N and braking time 1,200 seconds*

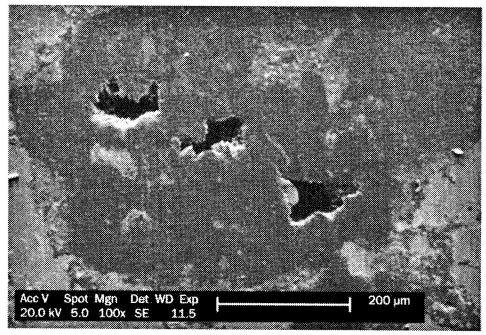

Figure 13. *Fatigue microcrack nucleated at the areas where pits and spalls were found. Applied load 100 N and braking time 720 seconds*

CONCLUSION

Based on the above observations, it can be concluded that the generation of fatigue mechanism depends on the applied load, braking time and type of braking mode. In continuous braking mode, it was found that fatigue mechanism only operated at an applied load of 200 N and below. However, in intermittent modes, it also operated under the applied load of 600 N. The process of fatigue mechanism generation was found to be manifested as follows; (i) generation of the plastic deformation due to cyclic contact during braking, (ii) formation of striations, whereby the spacing between striations became larger as the braking time was increased, (iii) nucleation of fatigue microcracks at the edges of transfer layer or at the areas where pits and spalls were present, (iv) propagation, growth and finally the joining of the microcracks to form loose particles before being disposed off from the worn surfaces.

ACKNOWLEDGEMENTS

The authors would like to thank the staff of Mechanical and Automotive Engineering Testing Unit and Metal Performance Centre, SIRIM Berhad for their cooperation and assistance in this study.

REFERENCES

ASM. (1992). *ASM Metal Handbook 11.* Failure and analysis prevention. Ohio, USA. American Society for Metals.

Bayer, R.G., Schumacher, R.A. (1968). On the significance of surface fatigue in sliding wear, Wear **12**, pp 173 - 183.

Bayer, R.G. (1994). Mechanical wear and prediction and prevention. New York: Marcel Dekker Inc.

Bros, J., Scieszka, S.F. (1977). The investigation of factors influencing dry fricition in brakes. Wear **34**: pp 131-139.

Klensil, M., Lukas, P. (1980). Fatigue of metallic materials. Amsterdam: Elsevier Scientific Publishing Company.

Rhee, S.K. (1974). Wear mechanism for asbestos-reinforced automotive friction materials. Wear **29**: pp 371-393.

Talib, R.J. (2001). Penelitian morfologi haus permukaan serta pukal bahan geseran automotif. Universiti Kebangsaan Malaysia.

Talib, R.J., Azhari, C.H. (2000). A quantitative evaluation of wear in semi-metallic automotive friction materials. In: Proc. 2nd International Conference on Advances in Strategic Technologies (ICAST), pp 859-868, Putra Jaya.

Talib, R.J. C.H. Azhari. (1997). Ciri geseran dan haus. *Journal of Industrial Tech.* **6** (1): pp 29-46.

Talib, R.J., K. Ramlan. C.H Azhari. (2002). Wear of friction materials for passenger cars. *J. Solid State Sc. & Tech.,* **10 (1,2)**, pp 292-298.

Talib, R.J. (1996). *Kajian mekanisme haus pad brek. Tesis Sarjana.* Universiti Kebangsaan Malaysia.